Energy Conversion and Management 76 (2013) 1073–1082

Contents lists available at ScienceDirect

Energy Conversion and Management

journal homepage: www.elsevier.com/locate/enconman

Utilization of oil palm tree residues to produce bio-oil and bio-char via pyrolysis

Faisal Abnisa *, Arash Arami-Niya, W.M.A. Wan Daud, J.N. Sahu, I.M. Noor

Department of Chemical Engineering, Faculty of Engineering, University of Malaya, 50603 Kuala Lumpur, Malaysia

ARTICLE INFO

Article history:
Received 2 July 2013
Accepted 22 August 2013

Keywords:
Pyrolysis
Bio-oil
Bio-char
Oil palm tree residues
Malaysia

ABSTRACT

Oil palm tree residues are a rich biomass resource in Malaysia, and it is therefore very important that they be utilized for more beneficial purposes, particularly in the context of the development of biofuels. This paper described the possibility of utilizing oil palm tree residues as biofuels by producing bio-oil and bio-char via pyrolysis. The process was performed in a fixed-bed reactor at a temperature of 500 °C, a nitrogen flow rate of 2 L/min and a reaction time of 60 min. The physical and chemical properties of the products, which are important for biofuel testing, were then characterized. The results showed that the yields of the bio-oil and bio-char obtained from different residues varied within the ranges of 16.58–43.50 wt% and 28.63–36.75 wt%, respectively. The variations in the yields resulted from differences in the relative amounts of cellulose, hemicellulose, lignin, volatiles, fixed carbon, and ash in the samples. The energy density of the bio-char was found to be higher than that of the bio-oil. The highest energy density of the bio-char was obtained from a palm leaf sample (23.32 MJ/kg), while that of the bio-oil was obtained from a frond sample (15.41 MJ/kg).

© 2013 Elsevier Ltd. All rights reserved.

1. Introduction

Malaysia is a tropical and humid country located in the central part of Southeast Asia with a total landmass of 329,847 km^2. Approximately 24% of the nation's landmass is used by the agricultural sector, which means the land is categorized as arable, under permanent crops, and under permanent pastures [1]. Most of the land is planted with oil palm. The expansion of oil palm plantations has occurred each year over the last three decades at a real growth rate of 0.36% per year [2]. In 2010, it is estimated that approximately 48,537 km^2 (4,853,766 ha), or 14.72% of the total landmass, was used for oil palm plantations [2], with approximately 135–145 trees planted per hectare [3]. Each of the trees produces approximately 10% of palm oil, while the remaining 90% is biomass residue [4]. The different types of residues are produced by the mill and plantation activities. The palm kernel shells (PKS), mesocarp fibers (MF), and empty fruit bunches (EFB) are the main residues produced during the milling process, while the fronds and trunks are the major residues obtained from the plantation during felling. The fronds are also obtained during harvesting and pruning. The sources and types of residues are shown in Table 1. The volume and type of oil palm residues are expected to rapidly increase and will become a serious problem in the future.

Currently, the residues of the oil palm are the main contributors to biomass waste in Malaysia, and these wastes require extra attention with respect to handling. A survey of the literature indicates that most of them are handled with unsatisfactory practices that negatively impact the environment. Most of the residues from the plantations are incinerated or dumped as organic fertilizer to decompose naturally, and only 40% of the trunks are used in plywood manufacturing [3]. In palm oil mills, the PKS, EFB, and MF residues are generally sent to the boiler to be burned as fuel for steam generation [5]. Although burning the residues as fuel reduces the diesel consumption, this approach is not an environmentally friendly approach because it produces smoke and dust emissions due to incomplete combustion.

The abundant amount of biomass residue from oil palm can potentially be used as a renewable energy source through conversion into other energy products such as biofuel. The use of biomass in other forms of energy products is more beneficial than the direct burning of biomass because it releases many pollutants into the air. One potential technique for alleviating these environmental concerns is to convert oil palm residues into bio-oil and bio-char via pyrolysis. According to the literature, pyrolysis has been recommended as an environmentally friendly method because no wastes are produced during the process. Pyrolysis is the thermal decomposition of organic material at elevated temperatures in an inert environment, and the products of this process include bio-oil, bio-char, and syngas.

---

* Corresponding author. Tel.: +60 162709281; fax: +60 379675319.

E-mail addresses: faisal.abnisa@gmail.com (F. Abnisa), arash_araminiya@yahoo.com (A. Arami-Niya), ashri@um.edu.my (W.M.A. Wan Daud), jay_sahu@yahoo.co.in (J.N. Sahu), ishnoor2011@um.edu.my, ishnoor2010@gmail.com (I.M. Noor).

0196-8904/$ - see front matter © 2013 Elsevier Ltd. All rights reserved.
http://dx.doi.org/10.1016/j.enconman.2013.08.038

Table 1
Sources and types of oil palm residues.

Source of residue	Type of residue	Weight of the total source (%)	Quantity per hectare (ton/ha)
Fresh fruit bunch (from palm oil mill)	Palm kernel shell	5.5	1.10
	Empty fruit bunch	22	4.42
	Mesocarp fiber	13.5	2.71
Oil palm tree at felling (from plantation)	Trunk[a]	70	41.07
	Frond	20.5	16
	Leaf	6.53	7.69
	Other	2.97	19.44
Oil palm tree at pruning (from plantation)	Frond[b]	27.03	10.40

[a] Palm trunks felled once every 25–30 years.
[b] Consists of the leaf and measured in dry weight.

Bio-oil is the main product from pyrolysis because it is typically obtained in higher yields than the other products. The oil is formed from vapor condensation [6], and for biomass pyrolysis, the vapors are generally released at a temperature of 400–500 °C [7,8]. The oil obtained from the condensation process is dark brown in color and free-flowing and also has a strong acrid smell. Some advantages of bio-oil include ease of storage and transportation and use in the production of renewable energy and chemical feedstocks. According to Zheng, the energy density of bio-oil is four to five times higher than that of the original precursor, which offers important logistical advantages [9]. For chemical applications, the oil can be used to produce useful chemicals by taking advantage of its most abundant functional groups, such as carbonyl, carboxyl, and phenolic groups, through reaction or separation techniques [10,11].

In addition to liquid fuel, the stored solar energy of biomass can be converted into solid and gaseous fuels with high calorific values through pyrolysis and used for industrial combustion purposes [12]. The produced bio-char can be used as a highly efficient fuel in boilers either alone or as a mixture with biomass. In our previous study, we have shown that the bio-chars produced from the pyrolysis of palm oil wastes have high heating values of approximately 20–30 MJ/kg, which is comparable to those of some coals [13]. This value-added product is beneficial for soil amendment and prevents water contamination and soil erosion. Due to the high adsorption capacity of bio-char, it can adsorb moisture and nutrients and slowly release them to soil [14,15]. Bio-char can be used as a stable, renewable and inexpensive catalyst for biogas reforming and the conversion of greenhouse gases (CO_2 and CH_4) to value-added products [16–18]. Another application of bio-char is its use as an adsorbent in water treatment to remove heavy metals such as lead, cadmium, arsenic and chromium [19,20].

In the present work, the oil palm residues were characterized and then pyrolyzed in a fixed-bed reactor. The scope of this paper is limited only to residues from plantation activities, while the residues from mill activities were discussed previously [13]. All of the experiments were conducted at the same pyrolysis conditions to obtain the yields of bio-oil and bio-char. Furthermore, the chemical and physical properties of the products were characterized using several laboratory techniques.

2. Materials and methods

2.1. Raw materials

The oil palm wastes were obtained from Sime Darby Plantation in Selangor Dahrul Ehsan, Malaysia. The waste was separated into four samples categorized as trunk, frond, palm leaf, and palm leaf rib. Fig. 1 shows the wastes generated from oil palm trees. The samples were initially treated by washing and subsequent drying in the sun for 1 day. The dried samples were ground and screened to obtain particle sizes that ranged from 1.0 to 2.0 mm. Prior to use in the experiments, the samples were dried again in an oven at 105 °C for 24 h to remove the moisture.

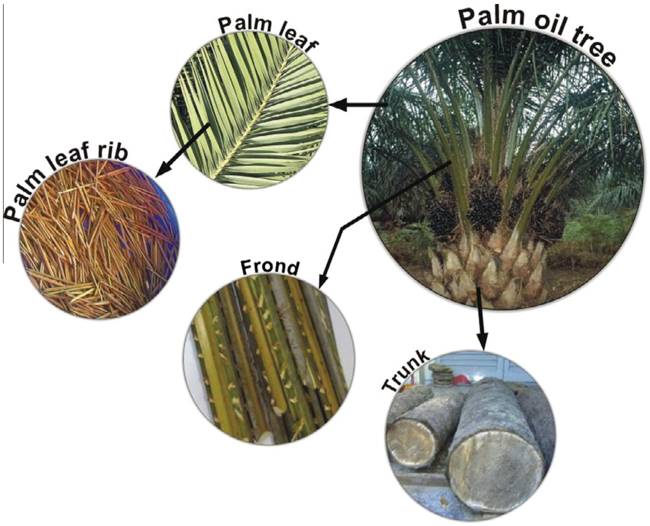

Fig. 1. The residues generated from oil palm trees.

2.2. Pyrolysis experiments

Approximately 200 g of the sample was placed in a stainless steel reactor with a length of 127 cm and an internal diameter of 2.5 cm. The fixed-bed reactor was selected in this study because it is relatively inexpensive, simple, and reliable [21]. An electric furnace was used to heat the reactor, and the temperature was monitored using a K-type thermocouple placed inside the reactor. A detailed design of the pyrolysis apparatus is shown schematically in Fig. 2. Nitrogen gas (N_2) was used as an inert gas to purge air from inside the reactor. Moreover, N_2 was also employed to sweep the vapor products from the reactor into the condensation traps. The purging with N_2 was performed throughout the entire procedure. The condensable products, specifically the bio-oils, were collected in a series of condensers and stored at 0.5 °C. They were subsequently weighed to obtain the mass of bio-oil. The bio-char was collected from the inside of the reactor and weighed. The final yields of bio-oil and bio-char were calculated using the following equation:

$$Y_{OP} = \frac{X_1}{X_2} \times 100\% \quad (1)$$

where Y_{OP} is the product yield, X_1 is the mass of the desired product, and X_2 is the initial mass of the raw material. The gas yield was determined by difference: gas yield = 100 − (bio-oil yield + bio-char yield).

In this study, the same parameters were employed for all of the experiments. Pyrolysis parameters were selected according to the literature studies [7,22] and the results from our previous study [23]. The experiments were conducted using a pyrolysis temperature of 500 °C, a particle size of 1–2 mm, a reaction time of 60 min, and an N_2 flow rate of 2 L/min. The heating rate was 10 °C/min. To validate the experimental data, each experiment was repeated with 3–5 replicates, and the average result was used as the final yield. The reactor, condenser, and piping system were sterilized between each set of experiments to avoid contamination of the samples.

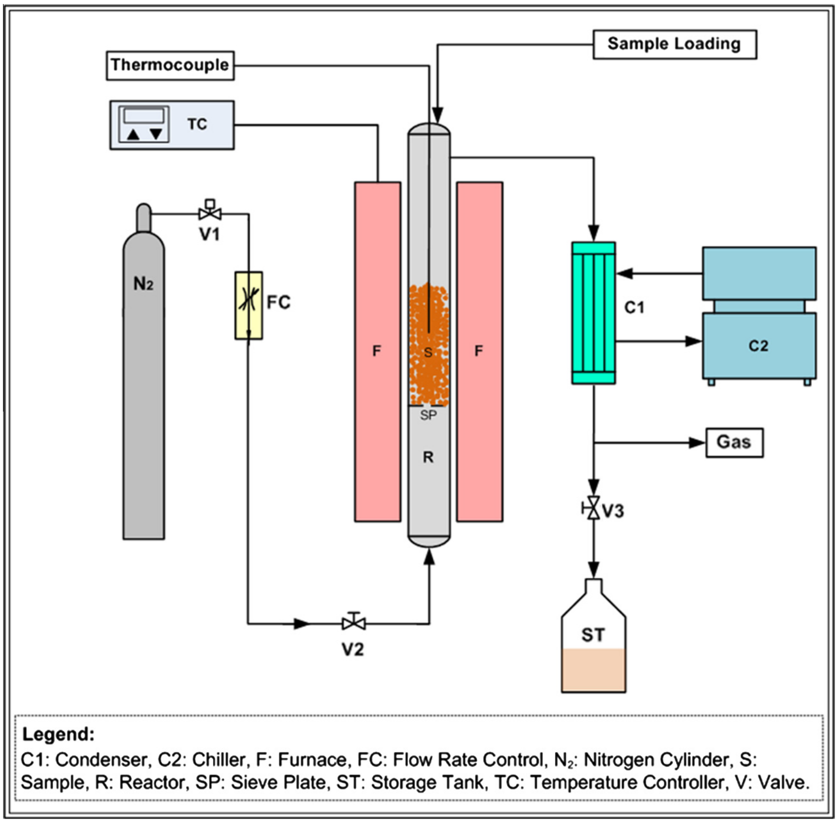
Sample Loading
Thermocouple
TC
N2
V1
FC
F
S
F
SP
R
C1
C2
Gas
V3
ST
V2
Legend:
C1: Condenser, C2: Chiller, F: Furnace, FC: Flow Rate Control, N2: Nitrogen Cylinder, S: Sample, R: Reactor, SP: Sieve Plate, ST: Storage Tank, TC: Temperature Controller, V: Valve.

Fig. 2. Schematic diagram of experimental setup.

2.3. Characterization

Prior to characterization, all feedstock were dried in an oven at a temperature of 105 °C for 24 h. The pyrolysis products from the experiments were collected in three different groups, bio-oil, bio-char, and syngas. Bio-oil and bio-char were collected and weighted directly after the production process and the amount of non-condensable gases were calculated by mass balance in the system. Before analysis, the bio-oil was separated into two fractions by a centrifugation process based on a procedure developed by Bertero et al. [24]. The process entailed centrifugation at 3200 rpm for 8 min, and the fractions after centrifugation are referred to as upper-layer bio-oil and bottom-layer bio-oil. In addition, in order to reduce the margin of error and to produce more reliable data, the analysis of each product from all experiments was repeated three times, and the results were averaged.

2.3.1. Physical characterization

The viscosity of the bio-oil was determined using a rotational viscometer equipped with an SC4-18 spindle (Brookfield Viscometer made in USA, model DV-II+Pro EXTRA). The measurement, which required approximately 7 mL of the sample, was taken at 50 °C. A 25 mL pycnometer was used to determine the density of the bio-oil. The measurement was performed by carefully filling the pycnometer with the oil and then measuring the mass. The density was determined by dividing the mass of the bio-oil by the empty volume of the pycnometer. The analysis was conducted at 24 °C. Scanning electron microscopy (SEM) experiments were conducted to study the physical morphology of the surfaces. A JSM-6390LV (JEOL, Japan) operating at a 3 kV accelerating voltage was used to characterize the morphology of the precursor and the bio-chars, which were dried overnight at approximately 105 °C under vacuum before SEM analysis. No conductive coating was applied to prepare the samples for SEM.

2.3.2. Chemical characterization

A Metrohm 827 pH meter (Switzerland) was used to analyze the pH of the bio-oils, and the measurements were performed at room temperature. The water content of the bio-oil was measured using a Karl Fischer 737 KF coulometer from Metrohm. Approximately 80 mL of Hydranal-Coulomat AG was used as the anolyte reagent, and 5 mL of Hydranal-Coulomat CG was used as the catholyte reagent. Approximately 2–6 mg of the pyrolytic liquid was injected through a titration cell into a flask.

The proximate analysis of both the precursors and the products were conducted according to ASTM D 7582-10 using thermal gravimetric analysis (TGA), and the results were expressed in terms of moisture, volatile matter, fixed-carbon and ash contents. The ultimate analysis was performed using a Model 2400 Series II CHNO/S analyzer (Perkin–Elmer, USA) to determine the C, H, and N contents. A CHN combustion tube and reduction tube were used for this measurement. As reported in the literature [23,25], oil palm wastes have very low sulfur content (around 0.1 wt%), thus, the value of it was not determined in this study. The oxygen content was determined by difference as following: $O = 100 - (C + H + N)$. The lignocellulosic contents of oil palm residues were determined using a method developed by Omar et al. [26]. In this method, three different analyses, namely acid detergent fiber (ADF), neutral detergent fiber (NDF), and acid detergent lignin (ADL), were performed. The final ADF, NDF, and ADL values were then used to calculate the percentage of cellulose, hemicellulose and lignin using the following equations [26]:

$$\text{Cellulose}(\%) = \text{ADF} - \text{ADL} \tag{2}$$

$$\text{Hemicellulose}(\%) = \text{NDF} - \text{ADF} \tag{3}$$

$$\text{Lignin}(\%) = \text{ADL} \quad (4)$$

The data obtained from the ultimate analysis were also used to calculate the high heating value (HHV). Eq. (5) was used to calculate the HHV because the oxygen content in the precursors and the products was found to be greater than 15% [27].

$$\text{HHV (MJ/kg)} = 0.336\ \text{C} + 1.418\ \text{H} - (0.153 - 0.000720\ \text{O})\text{O} + 0.0941\ \text{S} \quad (5)$$

To analyze the functional group compositions of the raw materials, bio-oils, and bio-chars, a FTIR spectrometer (Spectrum 400, Perkin–Elmer, USA) was used to collect the infrared (IR) spectra of the samples. The samples were scanned over the range from 400 to 4000 cm^{-1} with a resolution of 4 cm^{-1}. For the FTIR analysis, the raw materials and bio-chars were prepared using the following method. The sample (0.1 g) was mixed with 1 g of spectroscopy grade KBr in a porcelain mortar. The mixed sample was converted into a solid disk, which was placed in an oven at 105 °C for 4 h to avoid any interference with any existing water vapor or carbon dioxide molecules. A solid disk of pure KBr was used as a reference sample for background measurements.

3. Results and discussion

3.1. Characterization of the feedstock

The major components of the residues include cellulose, hemicellulose, and lignin; therefore, the thermal effect of the decomposition of these components plays an important role in the pyrolysis process to produce bio-oil and bio-char. Table 2 shows the lignocellulosic contents of the trunk, frond, palm leaf, and palm leaf rib, which were analyzed using the ADF, NDF, and ADL approaches. The three components decomposed at different rates and within distinct temperature ranges during the pyrolysis. According to Ishak et al. [28], hemicellulose decomposes first, and the decomposition of cellulose and then lignin follows. These phases were identified as the temperature increased during the pyrolysis. The hemicellulose usually starts to decompose near 220 °C, and the process is mostly complete by the time the temperature reaches 315 °C [29]. When hemicellulose had completely decomposed, cellulose then undergoes decomposition, which normally starts at a temperature of 315 °C and is completed at 400 °C. This temperature range can also be assigned to the second phase of the lignocellulosic decomposition. In this study, the frond had the highest cellulose content, while the trunk had the highest hemicellulose content. Both the cellulose and hemicellulose contributed significantly to the bio-oil yield [30].

Table 2
The lignocellulosic contents of oil palm tree residues.

Type of oil palm wastes	ADF	NDF	ADL	Cellulose (%)	Hemicellulose (%)	Lignin (%)
Trunk	70.33	94.27	35.89	34.44	23.94	35.89
Frond	72.03	95.21	21.7	50.33	23.18	21.7
Palm leaf	58.49	81.46	26	32.49	22.97	26
Palm leaf rib	75.41	98.58	29.31	46.1	23.17	29.31

The thermal behavior of lignin was found to be considerably different than that of hemicellulose or cellulose. Naturally, lignin has a more complex chemical composition; therefore, high-temperature conditions are necessary to decompose the lignin. The decomposition of lignin occurred slowly, starting at ambient temperature and proceeding up to a temperature of 900 °C [29]. In agreement with the literature, the lignin is responsible for the major portion of the bio-char product [30,31]. According to the results listed in Table 2, the trunk material had the highest lignin content in this study.

The proximate and ultimate analysis results for the different residues of oil palm waste are presented in Table 3. In this study, the proximate analysis has been used to quantify the relative proportions of moisture, volatiles, fixed carbon and ash in all the residues. The moisture content, which can be easily removed by drying the residue at a temperature of 105 °C overnight in an oven, was observed to be the highest for the frond residue. The percentage of volatile matter was found to be high for the frond and trunk, while the palm leaf and palm leaf rib were observed to have lower amounts. In contrast to the results for the volatile matter, the trunk and frond contained lower amounts of fixed carbon, 4.97 wt% and 3.22 wt%, respectively, than the palm leaf (11.92 wt%) and palm leaf rib (11.79 wt%). During pyrolysis, the presence of volatiles favors the production of a large amount of bio-oil. According to Omar et al. [26], the high volatiles content results in high volatility and reactivity, which are favorable for liquid fuel production. The temperature and heating rate significantly affected the volatile matter yield [32]. In addition, ash also plays an important role in determining the proportions of the products of biomass pyrolysis. An increase in the ash content contributes to a decrease in the bio-oil yield, and as consequence, the bio-char and non-condensable gases are produced in higher yields [33]. The effect of ash was clearly observed for the palm leaf, which had higher product yields of bio-char and non-condensable gases than that of bio-oil.

As listed in Table 3, the results from the ultimate analysis showed that all the materials contain similar amounts of C, H, N, and O. The C, H, N, and O contents of the oil palm residues varied as follows: carbon 40.40–43.76 wt%, hydrogen 5.58–6.30 wt%, nitrogen 0.38–1.94 wt%, and oxygen 49.57–52.09 wt%. The oxygen content was found to be higher than the C, H, and N contents of the oil palm residues, and the palm leaf has been confirmed to have the highest oxygen content of all the materials.

The infrared spectra of the raw materials are presented in Fig. 3. Various bands in the spectra were identified, including (1) O—H stretching vibrations at 3600–3100, 1333, and 1108 cm^{-1} and O—H bending at 1440–1400 cm^{-1} from acid and methanol compounds; (2) aromatic CH_n vibrations at 2970–2860, 1402, and 900–700 cm^{-1}; (3) C═O stretching at 1730–1700 and 1560–1510 cm^{-1}, C—O stretching at 1279–1060 cm^{-1}, aryl–alkyl ether

Table 3
Proximate and ultimate analyses of oil palm tree residues.

Type of palm oil wastes	Proximate analysis (wt%)				Ultimate analysis (wt%)			
	Moisture	Volatiles	Fixed carbon	Ash	C	H	N	O[a]
Trunk	7.16	82.60	4.97	5.27	42.72	5.61	0.44	51.24
Frond	13.84	82.70	3.22	0.24	42.76	5.99	0.39	50.88
Palm leaf	9.00	66.76	11.92	12.32	40.40	5.58	1.94	52.09
Palm leaf rib	8.01	75.94	11.79	4.26	43.76	6.30	0.38	49.57

[a] By difference.

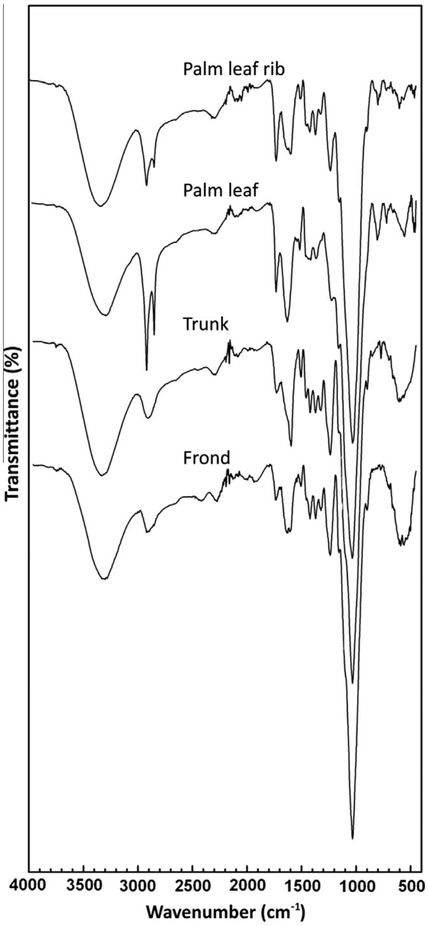

Fig. 3. FTIR spectra of oil palm residues.

linkage (1232 cm^{-1}) and pyranose ring skeletal C—O—C stretching (1170 and 1082 cm^{-1}); (4) benzene stretching of the ring C=C at 4632 cm^{-1} and aromatic C=C at 1613 and 1450 cm^{-1}; and (5) other groups such as C—O stretching at 1060 cm^{-1} and C—C stretching at 700–400 cm^{-1} [7,26,29]. The spectra of all the biomasses have similar shapes and intensities, although there are some small differences in their spectra. Just as for palm oil wastes, these biomasses also exhibit a significant IR absorbance at 1060 cm^{-1}, which might result from the presence of ethanol in their structures [13].

3.2. Bio-oil

3.2.1. Bio-oil yield

The results for the pyrolysis products listed in Table 4 show that the non-condensable gases are found in higher quantities than the bio-oils in the palm leaf and palm leaf rib. The lower oil yield is due to high ash content in the raw materials as shown in Table 3. The same trend also can be observed in the work published by Fahmi et al. [34]. They recognized that the presence of ash (alkali metals) decreases the yield of organic liquids and tends to increase char and gas yields. Moreover, the volatile matter also significantly affects the proportion of the bio-oil product. Asadullah et al. [35] noted that the volatile matter is usually converted to bio-oil upon condensation. Thus, it can be assumed that the smaller amount of volatile matter found in the palm leaf and palm leaf rib is responsible for the decrease in the amount of bio-oils. The smallest amount of bio-oil obtained was approximately 16.58 wt% for the palm leaf, which was composed of 66.76 wt% volatile matter and 12.32 wt% ash content.

Table 4
Product distributions from the pyrolysis of oil palm tree residues at a temperature of 500 °C, particle size of 1–2 mm, reaction time of 60 min, and N_2 flow rate of 2 L/min.

Type of oil palm wastes	Pyrolysis products (wt%)		
	Bio-oil	Bio-char	Non-condensable gases[a]
Trunk	40.87	33.60	25.53
Frond	43.50	30.24	26.26
Palm leaf	16.58	36.75	46.67
Palm leaf rib	29.02	28.63	42.35

[a] By difference.

The lignocellulosic nature of biomass is an important factor that affects the bio-oil yield. As shown in Table 4, a high oil yield was only observed for the trunk (40.87 wt%) and frond (43.50 wt%) samples. The higher bio-oil yield might be due to the fact that both samples have high cellulose and hemicellulose contents. Cellulose and hemicellulose promote the production of bio-oil because they are highly volatile. According to Qu et al. [36], cellulose is more volatile than hemicellulose. Therefore, the material with the largest amount of cellulose should have the most volatile matter, leading to an increase in the oil yield. In this study, the frond had the most cellulose (50.33%). The frond material also produced the most oil and had the largest amount of volatile matter (43.50 wt% and 82.70 wt%, respectively). The same tendencies were found by Mullen et al. for the fast pyrolysis of two corn residues, corn cobs, and corn stover [15]. Their research concluded that the highest bio-oil yield was observed for corn stover material, which has the highest cellulose content. In addition, the amount of the bottom-layer oil obtained from the centrifugation process was similar for all the samples and was in the range of 3–8 wt% of the total oil.

The result from our previous study [13] showed that the yields of bio-oils obtained were approximately 47.43 wt%, 45.75 wt%, and 43.87 wt% for palm shell, empty fruit bunches, and mesocarp fiber, respectively. Therefore, it can be concluded that the yields of bio-oils from the residues of palm oil mill activities is more attractive than those of residues from plantation activities.

3.2.2. Characterization of the bio-oils

The bio-oil properties are summarized in Table 5. From Table 5, it can be observed that the measured water contents were high, ranging from 52 to 66 wt%, for all bio-oils. This result is consistent with the results reported by Bertero et al. [24]. In their research, sawdust pine, mesquite trees, and wheat shell were pyrolyzed at a temperature of 550 °C for 60 min, and the water contents were determined to be within the range of 49.60–84.40 wt%. Wasterhof et al. [37] have studied how to control the water content of biomass fast-pyrolysis oil, and they have concluded that drying the feedstock to obtain very low moisture levels (approaching zero) leads to a decrease in the water content. On the other hand, Garcia-Perez et al. [38] stated that the biomass particle size has a significant effect on the water content of bio-oil. Generally, a smaller particle size increases the water content. While a high water con-

Table 5
Properties of bio-oils produced via the pyrolysis of oil palm tree residues.

Type of bio-oil	Properties			
	Water content (wt%)	Viscosity at 50 °C (cP)	Density (kg/m^3)	pH
Trunk	52	1.99	1053	3.1
Frond	53	1.88	1045	2.1
Palm leaf	59	1.75	1040	3.8
Palm leaf rib	66	1.23	1034	4.6

tent decreases the viscosity of bio-oil, which is helpful for pumping purposes, water is an undesirable component of bio-oil because it can be detrimental for the ignition performance.

The viscosities of the bio-oils were found to range from 1.23 to 1.99 cP at 50 °C. In this study, the viscosity exhibited a negative linear relationship with the water content. As shown in Table 5, an increase in the water content reduces the oil viscosity. These results are in agreement with the work of Nolte et al. [39], which investigated the viscosity of biomass pyrolysis oils from various feedstocks. Furthermore, the viscosity of oil can increase during the storage time. According to Diebold and Czernik [40], the viscosity of an oil increases because of the polymerization of the reactive species, and as consequence, it might become unstable and separate into two phases (a viscous bottom portion and a fluid aqueous upper portion) [41].

The presence of water in bio-oil also affects the density. Typically, a high water content leads to a decrease in the bio-oil density [42]. This trend is clearly observed in this study where the oil produced from palm leaf rib has the highest water content and the lowest density compared to the other bio-oil samples. Several researchers have supported this finding with studies using various biomass pyrolysis process conditions. Salehi et al. [43] found that the density of bio-oil obtained from the pyrolysis of sawdust in a fixed-bed system is 1050 kg/m^3 at a water content of 39%. Lu et al. [44] studied the chemical and physical properties of bio-oil produced via the fast pyrolysis of rice husk, and they measured an oil density of 1140 kg/m^3 at 28% water content. Zheng et al. [45] obtained an oil density of 1160 kg/m^3 at a water content of 24.2%. The oil was produced from the fast pyrolysis of cotton stalk at a temperature of 510 °C in a fluidized bed reactor.

The pH values for all bio-oils obtained from the pyrolysis of oil palm residues were in the range of 2.1–4.6. In general, the low pH is due to the high concentration of acidic compounds in bio-oil. According to Sınağ et al. [46], a high concentration of acidic compounds might result from the degradation of hemicellulose and lignin during pyrolysis. The low pH makes the oil highly unstable and corrosive. Therefore, careful material selection is needed in the design of storage and piping systems.

Fig. 4a shows the bio-oil spectra from the FTIR analysis. The results showed that all the bio-oils have similar types of chemical bonds (functional groups). The strong absorption peaks observed between 3200 and 3600 cm^{-1} indicate that phenols and alcohols are present. On the other hand, the peaks are also considered to result from the presence of water impurities [47]. This finding is consistent with the results in Table 5, namely that the water content of the bio-oils was found to be large in this study. The absorption peaks in the range of 1650–1750 cm^{-1}, which are related to C═O stretching, indicate the presence of ketones, carboxylic acids, and aldehydes. However, only the oil produced from palm leaf rib does not exhibit obvious peaks in this range. The —C—H bending vibrations between 1350 cm^{-1} and 1480 cm^{-1}, which indicate the presence of alkanes, were observed for all of the bio-oils. Moreover, the acid compounds are represented by the C—O stretching peaks observed between 1210 cm^{-1} and 1320 cm^{-1}. From Fig. 4a, it can be seen that the oils from the trunk, frond, and palm leaf exhibited stronger peaks, indicating that they are more acidic than the oil produced from the palm leaf rib. This finding is in good agreement with the pH analysis results listed in Table 5. The C—O stretching vibrations in the range of 970–1150 cm^{-1} were assigned to alcohol and phenolic groups. The peaks in the range of 600–700 cm^{-1} showed that alkynes, which are represented by the C—H bending vibration, were present.

Table 6 presents the ultimate analysis results for the upper-layer bio-oils. The results showed that more than 70% of the oxygen was detected in the upper layer of the bio-oils. The high level of oxygen is generally found in bio-oils produced from the pyrolysis of biomass. Several authors have reported the oxygen content in varying types of biomass to range from 35 to 60 wt% [11,48,49]. However, the oils produced in this work have a higher oxygen content than has been previously reported in the literature. In this case, additional ultimate analyses were performed on the bottom-layer products in order to further investigate the behavior of the oxygen content. As shown in Table 6, the bottom-layer bio-oil products have less oxygen than the upper-layer products. The bottom-layer product of the palm leaf rib residue has the highest oxygen content of 49.16 wt%. In contrast to the upper-layer products, a high carbon content was measured for all bottom-layer

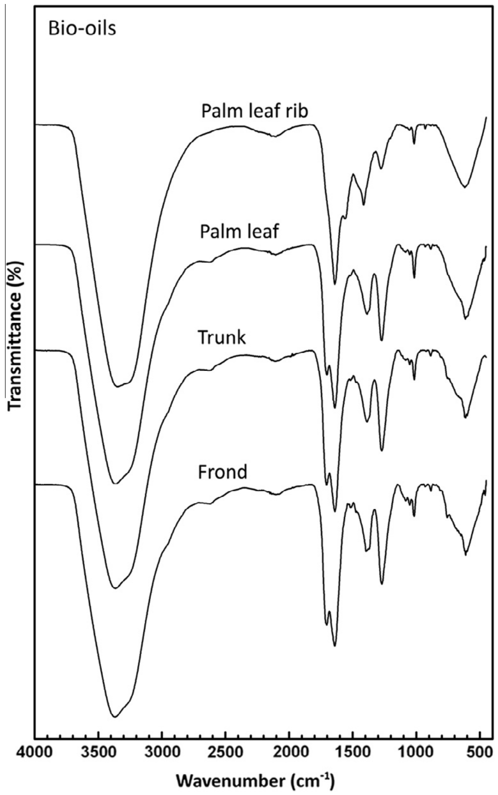

Fig. 4a. FTIR spectra of bio-oils.

Table 6
Ultimate analysis and HHV results.

Type of product	Type of oil palm residue			
	Trunk	Frond	Palm leaf	Palm leaf rib
Bio-oil (upper layer)				
C (wt%)	16.88	17.93	15.16	10.34
H (wt%)	11.64	11.69	11.70	9.60
N (wt%)	0.64	0.33	0.65	1.64
O[a] (wt%)	70.85	70.07	72.48	78.42
HHV (MJ/kg)	14.94	15.41	14.38	9.52
Bio-oil (bottom layer)				
C (wt%)	50.56	54.57	55.54	39.66
H (wt%)	9.82	9.03	7.69	7.13
N (wt%)	1.07	0.63	3.60	4.06
O[a] (wt%)	38.56	35.77	33.17	49.16
HHV (MJ/kg)	24.31	25.03	23.90	14.83
Bio-char				
C (wt%)	63.68	65.33	71.79	49.60
H (wt%)	2.28	2.56	2.41	2.14
N (wt%)	0.63	0.75	1.27	2.74
O[a] (wt%)	33.43	31.37	24.54	45.53
HHV (MJ/kg)	18.79	20.12	23.32	11.64

[a] By difference.

products. A similar trend was also observed in the study conducted by Chen et al. [50], where they found that the bottom-layer bio-oil has high carbon and low oxygen contents, while the opposite was observed for the upper layer. This finding is supported by Samanya et al. [51], who noted that the upper layer contained lighter organic fractions, while the bottom layer contained tar fractions originating from wood. Of the four elements studied in the ultimate analysis, nitrogen was detected in the smallest quantities in the upper and bottom layers of the bio-oil.

The HHV of the bio-oil are listed in Table 6. The HHV of the upper-layer products, which were calculated using Eq. (5), were approximately 14.94 MJ/kg, 15.41 MJ/kg, 14.38 MJ/kg, and 9.52 MJ/kg for the trunk, frond, palm leaf, and palm leaf rib, respectively. However, these values are much lower than those reported by Czernik and Bridgwater [11], who measured HHV of approximately 16–19 MJ/kg. The high water and oxygen contents are mainly responsible for the low bio-oil HHV. Moreover, the results in Table 6 clearly showed that the HHV of the bottom-layer products were higher than those of the upper-layer products. The different carbon contents between the upper and bottom layers might explain the difference in the HHV listed in Table 6. Nevertheless, the hydrogen content in the upper layer of the bio-oil was similar to that of heavy fuel oil reported in the literature [11]. Hydrogen is the most important component with respect to increasing the HHV because it has the highest heating value among known fuels and is typically measured to be approximately 141 MJ/kg [52].

3.3. Bio-char

3.3.1. Bio-char yields

The product distributions from the biomass pyrolysis at 500°C are shown in Table 4. The palm leaf had the highest bio-char product yield, followed by the trunk, frond and finally palm leaf rib. The different behavior of the hemicellulose, cellulose and lignin components at the pyrolysis temperature affects the product yields. Hemicellulose starts to decompose over a low temperature range of 220–315 °C [29]; therefore, most of it decomposes at the pyrolysis conditions of this study. In addition, the hemicellulose content of all the precursors is similar (Table 2). Thus, the hemicellulose contents cannot be an important factor in the bio-char and non-condensable product yields. Lignin, which is composed of aromatic rings with various branches, decomposes over a wide range of low to very high temperatures with a very low mass loss rate [29]. Therefore, the samples with higher lignin content might have relatively higher bio-char yields [53], which is true in the case of the trunk sample. Although lignin content is an important parameter, cellulose content can be considered to be the most significant factor in determining the bio-char yield. We observed this effect in our last study where the biomass sample with the highest cellulose content, the EFB sample, had a high bio-char yield [13]. Due to a faster mass loss rate of cellulose (6.5 wt%/°C) than of other components, almost all of it would decompose at the pyrolysis temperature of this study. Therefore, the samples with high cellulose content will lose a large portion of their mass during pyrolysis, which might explain the lower bio-char yields of 30.24% and 28.63% for the frond and palm leaf rib samples, respectively, although they had the highest cellulose contents (46.1% for the frond and 50.33% for the palm leaf rib).

On the other hand, the palm leaf and trunk had very high carbon-based and volatile matter contents, respectively, in the precursor and bio-char samples (Table 3 and Fig. 5). The very high amount of fixed carbon in the palm leaf samples (raw material and bio-char) can explain the high bio-char yield. In the case of the trunk-based bio-char, which was the second highest yield, the low decomposition of the volatile content during the pyrolysis process in addition to a high lignin content can contribute to its high yield.

The sweeping gas removes the products of secondary reactions, such as thermal cracking, repolymerization, and recondensation, from the hot zone [54]. The part of this pyrolysis vapor that is condensed in the cooling apparatus is called bio-oil, and the other part is a non-condensable gas mixture that contains CO, CO_2, H_2, and CH_4. The gas product yields of the oil palm wastes are listed in Table 4. The palm leaf and palm leaf rib had the highest product yields of 46.7% and 42.3%, respectively. It was reported in the literature that a high gas yield can be attributed to a high hemicellulose content in the precursor [13,55]. However, the hemicellulose content of the precursors are similar in this study. As shown by the proximate analysis results for the produced bio-chars in Fig. 5, the bio-chars with fewer volatile residuals have higher non-condensable gas product yields. Both the palm leaf and palm leaf rib had the lowest volatiles content of 28.7% in the produced bio-chars and the highest non-condensable gas product yields. Conversely, the samples with high volatile matter content in their bio-char (trunk) had the lowest non-condensable gas product yields. Thus, it can be concluded that the samples with the highest decomposition of volatile matter have higher gas product yields.

3.3.2. Characterization of bio-chars

The FTIR spectra of the trunk, frond, palm leaf and leaf rib bio-chars are shown in Fig. 4b. Compared to the infrared spectra of the raw biomasses in Section 3.1, the spectra of these carbonaceous materials show that different oxygen-containing surface groups (C=O, C—O, —OH) and other groups (olefins, $—CH_2$, $—CH_3$, aromatic rings) are present. The O—H stretching vibrations at 3600–3100 cm^{-1} in the FTIR spectra of the produced bio-chars were nearly absent after the carbonization process, probably due to

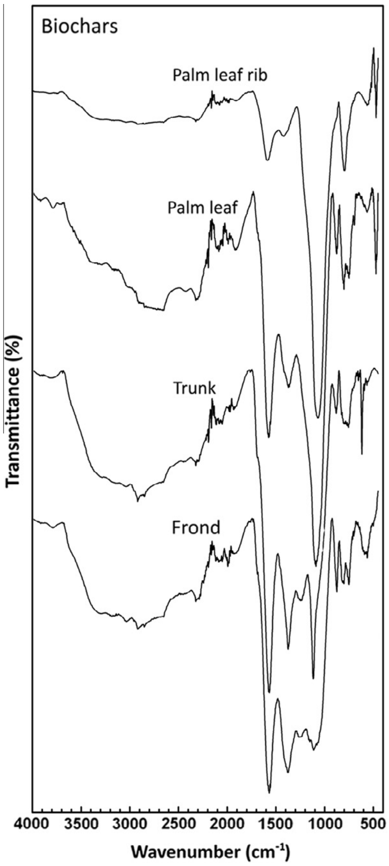

Fig. 4b. FTIR spectra of bio-chars.

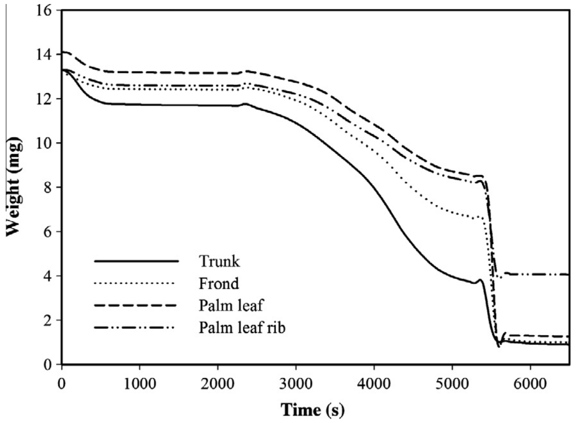

Fig. 5. Mass loss behavior of the produced bio-chars over time under nitrogen and then oxygen heating.

the dehydration of the biomass together with the release of a large amount of water [7]. A decrease in the intensity of the alkene (C—H) group vibrations in all three biomasses could be explained by the breaking of the weak alkyl C—H bonds, which would increase the CH_4 and C_2 hydrocarbon content in the gas products. However, in the case of the trunk-based bio-chars, a small IR absorption peak that is consistent with the proximate analysis data in Table 3 showing that the trunk samples contain a high level of volatiles after carbonization is observed. The next band in the spectra of the raw materials occurring at 2860–2970 cm^{-1}, which can be assigned to the CH alkyl functional groups, were also absent in the spectra of the biomass chars. The CH aromatic bands at 877.04–779.19 cm^{-1} were also weaker due to the deformation of the adjacent H. In addition, the intensity of the carboxyl group band at 1718.83 cm^{-1} decreased in all the bio-char samples, possibly due to the degradation of the cellulose components during pyrolysis.

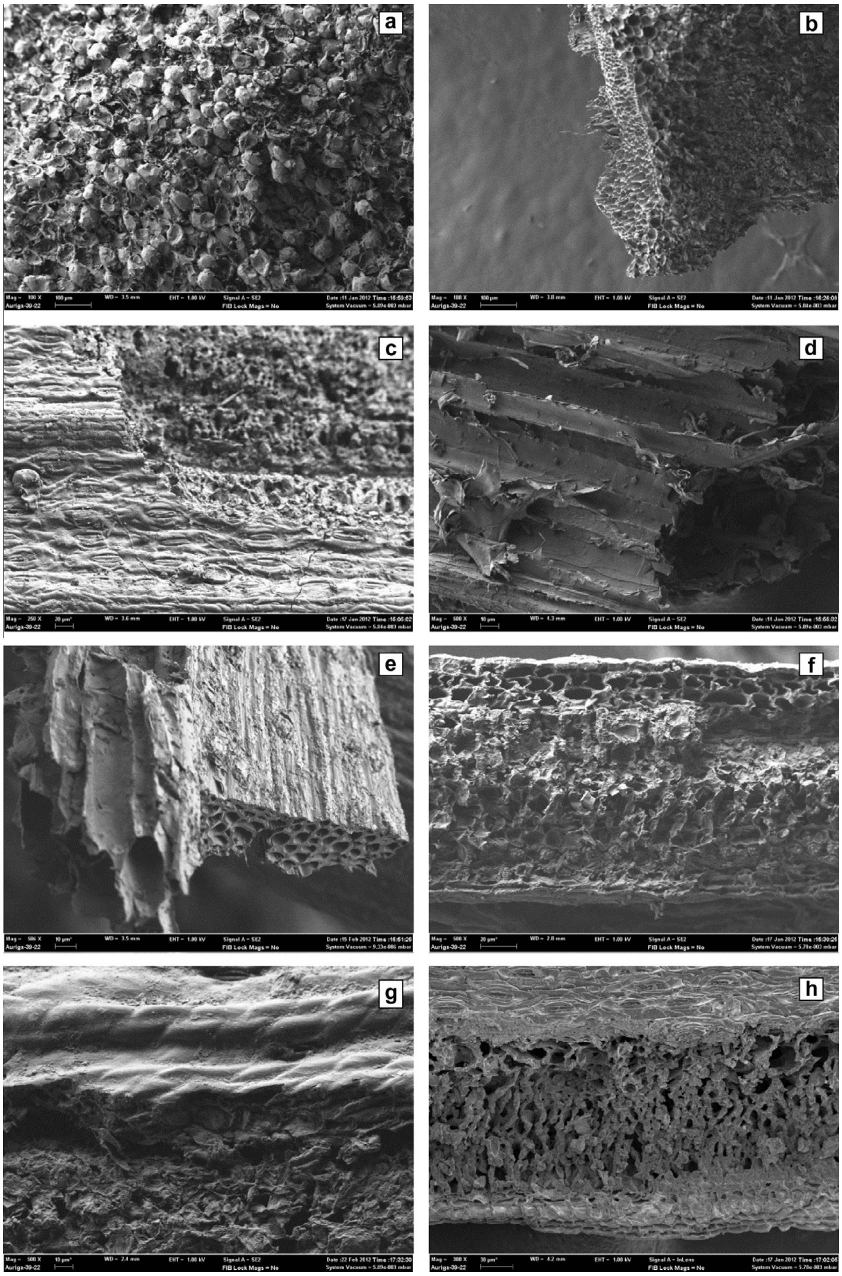

Fig. 6. SEM photographs of (a) trunk, (b) trunk bio-char, (c) frond, (d) frond bio-char, (e) leaf, (f) leaf bio-char, (g) rib, and (h) rib bio-char.

On the other hand, the FTIR spectral data indicate that the IR peaks of the produced chars at 2313–2330 cm^{-1} (C≡C) and 1586–1571.62 cm^{-1} (aromatic C=C) increased in intensity relative to those of the raw biomasses after the carbonization process. The cracking of volatiles (decrease in the OH and CH alkyl peaks) and the conversion of the aliphatic compounds into aromatic compounds in the char structure can explain these bands.

The proximate analysis of the produced bio-chars was performed according to ASTMD7582-10, and the results are summarized in Fig. 5. The moisture, volatiles, fixed-carbon and ash contents can be derived from the mass losses of the carboneous samples over the process time shown in Fig. 5. It can be seen that all the samples undergo three main mass losses. The first occurs during heating from room temperature to 110 °C under a nitrogen atmosphere, which leads to complete dehydration and thus allows for the determination of the moisture content (up to 2300 s). Then the temperature is increased rapidly to 950 °C to determine the amount of volatile matter by measuring the mass loss after dehydration (between 2300 and 4700 s). Finally, the temperature was decreased to 650 °C, and the atmosphere was changed to oxygen gas to measure the mass loss during the oxidation stage, which corresponds to the carbon content (rapid decrease in the mass of all the samples). Ash constituted the mass remaining at the end of the analysis. Based on this figure, the trunk-based char has the highest volatile content, followed by the frond, palm leaf and rib samples. However, the last two had similar volatile matter contents. Thus, it can be concluded that a higher carbonization temperature is needed in the case of the trunk-based bio-char to improve the devolatilization. The leaf char sample had the highest fixed-carbon content, which was similar to that of the frond-based sample, while the rib and trunk samples had much lower fixed-carbon contents. The ash content of all the samples is similarly low except in the case of the rib sample, which contained a very high amount of ash after carbonization.

The results of ultimate analysis of bio-char are listed in Table 6. The HHV of the produced bio-chars are also given in this table. Carbon, as the main element in all of the produced bio-chars (49–72 wt%), is present in significantly greater amounts in the bio-chars than in the dried biomasses, except for the palm leaf sample, which had similar amounts of carbon and oxygen before and after pyrolysis (see Table 3). In comparison to the raw biomasses, the O and H contents decrease in all the bio-char samples due to dehydration and decarbonylation/decarboxylation reactions, which is consistent with the FTIR results (Fig. 4b). The largest decrease in the O and H contents is observed for the palm leaf sample, which was found to have the second highest devolatilization percentage (approximately 57%) in the proximate analysis. Although the palm leaf rib exhibited the highest devolatilization (approximately 62%) during pyrolysis, possibly due to its high ash content in the produced bio-char, the amount of carbon and oxygen did not change considerably. The hydrogen content decreases in all the samples, probably due to the aromatization of the bio-char and evolution of H_2 as light molecular hydrocarbons (CH_4 and C_2) were formed during the pyrolysis process [29].

The HHV of the bio-char samples calculated using Eq. (5) is highly dependent on the hydrogen and carbon contents of the samples. As long as all the bio-char samples have similar hydrogen contents (2–3%), the amount of carbon plays an important role in the determination of HHV. Thus, similarly to the carbon content, HHV also follows the order of palm leaf > frond > trunk > palm leaf rib. With the exception of the palm leaf rib sample with a low HHV, the other bio-char samples have HHV values comparable to those of some coals and are therefore acceptable for use as a renewable solid fuel [56,57]. The low level of nitrogen content in the bio-char samples also indicates that these samples produce low levels of NO_x emissions during the combustion process.

Fig. 6 presents the SEM pictures of the raw biomasses and their bio-chars obtained after pyrolysis. It is clear in all the images that the pyrolysis of the biomasses allows the evolved volatile compounds to escape from the inside of the raw materials. Consequently, more void space and higher porosity are detectable on the surface of the bio-chars, which have higher surface areas than the raw materials. The images of the bio-chars show the heterogeneity of their surfaces with mesopores that can be useful in many liquid–solid adsorption processes [20]. As shown in Fig. 6, the primary surface structures changed during the carbonization and devolatilization processes. Spherical structures on the surface of the trunk (Fig. 6a) were transformed into open cells after carbonization (Fig. 6b), while the amorphous structure of the frond (Fig. 6c) allowed for the formation of open channels after devolatilization (Fig. 6d). Partly open channels and larger pores in the palm leaf and palm leaf rib bio-chars (Fig. 6f and h) are also observed after pyrolysis of the amorphous raw biomasses (Fig. 6e and g).

4. Conclusions

All of the residues that came from oil palm plantation activities have been successfully pyrolyzed to produce bio-oil and bio-char using a reaction temperature of 500 °C, a nitrogen flow rate of 2 L/min and a reaction time of 60 min. Different proportions of the products have been clearly observed in this study and are mainly caused by the different amounts of cellulose, hemicellulose, lignin, volatile matter, fixed carbon, and ash in the samples. The HHV of the upper layer of the bio-oils was found to range from 9.52 to 15.41 MJ/kg, while the HHV of the bottom layer was higher (approximately 14.83–25.03 MJ/kg). However, further efforts to improve the quality of the bio-oil must be performed prior to its use as an alternative fuel. The improvement can be performed through the catalytic cracking or hydrodeoxygenation process. Furthermore, most of the bio-char samples have HHV that are comparable to those of some coals and are thus acceptable for use as a renewable solid fuel. They also have low levels of NO_x emissions during the combustion process. In addition, the SEM images showed that the pyrolysis of the biomasses allows the evolved volatile compounds to escape from the inside of the raw materials and consequently increases the porosity of the surface of the produced bio-chars.

Acknowledgements

The authors would like to thank the University of Malaya for fully funding the work described in this publication through the Bright Sparks Program, the Postgraduate Research Grant, and the HIR Grants (D000011-16001).

References

[1] World Bank. Agricultural land (% of land area). <http://data.worldbank.org/indicator/AG.LND.AGRI.ZS> [accessed 17.09.12].
[2] Department of Statistics Malaysia. Malaysia economic statistics – time series 2011. ISSN 0127-9181.
[3] Asma IW, Mahanim S, Zulkafli H, Othman S, Mori Y. Malaysia oil palm biomass. Forest Research Institute Malaysia, Regional workshop on UNEP/DTIE/IETC in collaboration with GEC, Osaka Japan, 2–5 March; 2010.
[4] Hon LM. A case study on palm empty fruit bunch as energy feedstock. SEGi Rev 2010;3:3–15.
[5] Mahlia TMI, Abdulmuin MZ, Alamsyah TMI, Mukhlishien D. An alternative energy source from palm wastes industry for Malaysia and Indonesia. Energy Convers Manage 2001;42:2109–18.
[6] Zheng J-L, Kong Y-P. Spray combustion properties of fast pyrolysis bio-oil produced from rice husk. Energy Convers Manage 2010;51:182–8.
[7] Yang H, Yan R, Chen H, Lee DH, Liang DT, Zheng C. Mechanism of palm oil waste pyrolysis in a packed bed. Energy & Fuels 2006;20:1321–8.
[8] Gerçel HF. Bio-oil production from *Onopordum acanthium* L. by slow pyrolysis. J Anal Appl Pyrol 2011;92:233–8.

[9] Zheng J-L. Pyrolysis oil from fast pyrolysis of maize stalk. J Anal Appl Pyrol 2008;83:205–12.
[10] Fele Žilnik L, Jazbinšek A. Recovery of renewable phenolic fraction from pyrolysis oil. Sep Purif Technol 2012;86:157–70.
[11] Czernik S, Bridgwater AV. Overview of applications of biomass fast pyrolysis oil. Energy Fuel 2004;18:590–8.
[12] Lim MT, Alimuddin Z. Bubbling fluidized bed biomass gasification – performance, process findings and energy analysis. Renew Energy 2008;33:2339–43.
[13] Abnisa F, Arami-Niya A, Daud WMAW, Sahu JN. Characterization of bio-oil and bio-char from pyrolysis of palm oil wastes. BioEnergy Res 2013;6:830–40.
[14] Laird DA. The charcoal vision: a win-win-win scenario for simultaneously producing bioenergy, permanently sequestering carbon, while improving soil and water quality. Agron J 2008;100:178–81.
[15] Mullen CA, Boateng AA, Goldberg NM, Lima IM, Laird DA, Hicks KB. Bio-oil and bio-char production from corn cobs and stover by fast pyrolysis. Biomass Bioenergy 2010;34:67–74.
[16] Domínguez A, Fernández Y, Fidalgo B, Pis JJ, Menéndez JA. Biogas to syngas by microwave-assisted dry reforming in the presence of char. Energy Fuel 2007;21:2066–71.
[17] Dufour A, Celzard A, Fierro V, Martin E, Broust F, Zoulalian A. Catalytic decomposition of methane over a wood char concurrently activated by a pyrolysis gas. Appl Catal A – Gen 2008;346:164–73.
[18] Muradov N, Fidalgo B, Gujar AC, Garceau N, T-Raissi A. Production and characterization of *Lemna minor* bio-char and its catalytic application for biogas reforming. Biomass Bioenergy 2012;42:123–31.
[19] Mohan D, Pittman Jr CU, Bricka M, Smith F, Yancey B, Mohammad J, et al. Sorption of arsenic, cadmium, and lead by chars produced from fast pyrolysis of wood and bark during bio-oil production. J Colloid Interface Sci 2007;310:57–73.
[20] Mohan D, Rajput S, Singh VK, Steele PH, Pittman Jr CU. Modeling and evaluation of chromium remediation from water using low cost bio-char, a green adsorbent. J Hazard Mater 2011;188:319–33.
[21] Bridgwater AV. Renewable fuels and chemicals by thermal processing of biomass. Chem Eng J 2003;91:87–102.
[22] Bridgwater AV. Principles and practice of biomass fast pyrolysis processes for liquids. J Anal Appl Pyrol 1999;51:3–22.
[23] Abnisa F, Wan Daud WMA, Sahu JN. Optimization and characterization studies on bio-oil production from palm shell by pyrolysis using response surface methodology. Biomass Bioenergy 2011;35:3604–16.
[24] Bertero M, de la Puente G, Sedran U. Fuels from bio-oils: bio-oil production from different residual sources, characterization and thermal conditioning. Fuel 2012;95:263–71.
[25] Sulaiman F, Abdullah N. Optimum conditions for maximising pyrolysis liquids of oil palm empty fruit bunches. Energy 2011;36:2352–9.
[26] Omar R, Idris A, Yunus R, Khalid K, Aida Isma MI. Characterization of empty fruit bunch for microwave-assisted pyrolysis. Fuel 2011;90:1536–44.
[27] Buckley TJ. Calculation of higher heating values of biomass materials and waste components from elemental analyses. Resour Conserv Recycl 1991;5:329–41.
[28] Ishak MR, Sapuan SM, Leman Z, Rahman MZA, Anwar UMK. Characterization of sugar palm (*Arenga pinnata*) fibres. J Therm Anal Calorim 2012;109:981–9.
[29] Yang H, Yan R, Chen H, Lee DH, Zheng C. Characteristics of hemicellulose, cellulose and lignin pyrolysis. Fuel 2007;86:1781–8.
[30] Akhtar J, Saidina Amin N. A review on operating parameters for optimum liquid oil yield in biomass pyrolysis. Renew Sust Energy Rev 2012;16:5101–9.
[31] Zabaniotou A, Ioannidou O, Antonakou E, Lappas A. Experimental study of pyrolysis for potential energy, hydrogen and carbon material production from lignocellulosic biomass. Int J Hydrogen Energy 2008;33:2433–44.
[32] Guldogan Y, Bozdemir TO, Durusoy T. Effect of heating rate on pyrolysis kinetics of tuncbilek lignite. Energy Source 2000;22:305–12.
[33] Venderbosch RH, Prins W. Fast pyrolysis technology development. Biofuels Bioprod Biorefin 2010;4:178–208.
[34] Fahmi R, Bridgwater AV, Donnison I, Yates N, Jones JM. The effect of lignin and inorganic species in biomass on pyrolysis oil yields, quality and stability. Fuel 2008;87:1230–40.
[35] Asadullah M, Anisur Rahman M, Mohsin Ali M, Abdul Motin M, Borhanus Sultan M, Robiul Alam M, et al. Jute stick pyrolysis for bio-oil production in fluidized bed reactor. Bioresour Technol 2008;99:44–50.
[36] Qu T, Guo W, Shen L, Xiao J, Zhao K. Experimental study of biomass pyrolysis based on three major components: hemicellulose, cellulose, and lignin. Ind Eng Chem Res 2011;50:10424–33.
[37] Westerhof RJM, Kuipers NJM, Kersten SRA, van Swaaij WPM. Controlling the water content of biomass fast pyrolysis oil. Ind Eng Chem Res 2007;46:9238–47.
[38] Garcia-Perez M, Wang XS, Shen J, Rhodes MJ, Tian F, Lee W-J, et al. Fast pyrolysis of oil mallee woody biomass: effect of temperature on the yield and quality of pyrolysis products. Ind Eng Chem Res 2008;47:1846–54.
[39] Nolte MW, Liberatore MW. Viscosity of biomass pyrolysis oils from various feedstocks. Energy Fuel 2010;24:6601–8.
[40] Diebold JP, Czernik S. Additives to lower and stabilize the viscosity of pyrolysis oils during storage. Energy Fuel 1997;11:1081–91.
[41] Oasmaa A, Kuoppala E. Fast pyrolysis of forestry residue. 3. Storage stability of liquid fuel. Energy Fuel 2003;17:1075–84.
[42] Oasmaa A, Leppämäki E, Koponen P, Levander J, Tapola E. Physical characterisation of biomass-based pyrolysis liquids. Application of standard fuel oil analyses. Espoo: Technical Research Centre of Finland, VTT Publications 306; 1997.
[43] Salehi E, Abedi J, Harding T. Bio-oil from sawdust: pyrolysis of sawdust in a fixed-bed system. Energy Fuel 2009;23:3767–72.
[44] Lu Q, Yang X-l, Zhu X-f. Analysis on chemical and physical properties of bio-oil pyrolyzed from rice husk. J Anal Appl Pyrol 2008;82:191–8.
[45] Zheng J-l, Yi W-m, Wang N-n. Bio-oil production from cotton stalk. Energy Convers Manage 2008;49:1724–30.
[46] Sınağ A, Uskan B, Gülbay S. Detailed characterization of the pyrolytic liquids obtained by pyrolysis of sawdust. J Anal Appl Pyrol 2011;90:48–52.
[47] Das P, Sreelatha T, Ganesh A. Bio oil from pyrolysis of cashew nut shell-characterisation and related properties. Biomass Bioenergy 2004;27:265–75.
[48] Lu Q, Li W-Z, Zhu X-F. Overview of fuel properties of biomass fast pyrolysis oils. Energy Convers Manage 2009;50:1376–83.
[49] Zhang Q, Chang J, Wang T, Xu Y. Review of biomass pyrolysis oil properties and upgrading research. Energy Convers Manage 2007;48:87–92.
[50] Chen H-W, Song Q-H, Liao B, Guo Q-X. Further separation, characterization, and upgrading for upper and bottom layers from phase separation of biomass pyrolysis oils. Energy Fuel 2011;25:4655–61.
[51] Samanya J, Hornung A, Apfelbacher A, Vale P. Characteristics of the upper phase of bio-oil obtained from co-pyrolysis of sewage sludge with wood, rapeseed and straw. J Anal Appl Pyrol 2012;94:120–5.
[52] Ali I, Basit MA. Significance of hydrogen content in fuel combustion. Int J Hydrogen Energy 1993;18:1009–11.
[53] Dong C-q, Zhang Z-f, Lu Q, Yang Y-p. Characteristics and mechanism study of analytical fast pyrolysis of poplar wood. Energy Convers Manage 2012;7:49–59.
[54] Ertaş M, Hakkı Alma M. Pyrolysis of laurel (*Laurus nobilis* L.) extraction residues in a fixed-bed reactor: characterization of bio-oil and bio-char. J Anal Appl Pyrol 2010;88:22–9.
[55] Basu P. Chapter 3 – pyrolysis and torrefaction. Biomass gasification and pyrolysis. Boston: Academic Press; 2010. pp. 65–96.
[56] Bilgen S, Kaygusuz K. The calculation of the chemical exergies of coal-based fuels by using the higher heating values. Appl Energy 2008;85:776–85.
[57] Akkaya AV. Proximate analysis based multiple regression models for higher heating value estimation of low rank coals. Fuel Process Technol 2009;90:165–70.